Journal of Environmental Radioactivity 208-209 (2019) 106026

Contents lists available at ScienceDirect

Journal of Environmental Radioactivity

journal homepage: www.elsevier.com/locate/jenvrad

Increased uranium concentrations in ground and surface waters of the Swiss Plateau: A result of uranium accumulation and leaching in the Molasse basin and (ancient) wetlands?

Anja Pregler[a,d,*], Heinz Surbeck[b], Jost Eikenberg[a,1], Simon Werthmüller[c], Sönke Szidat[d,e], Andreas Türler[d]

[a] *Paul Scherrer Institute, Department for Radiation Safety and Security, 5232 Villigen PSI, Switzerland*
[b] *Nucfilm GmbH, Fineta 46, 1792 Cordast, Switzerland*
[c] *Schenker Korner Richter AG, Büttenenhalde 42, 6006 Luzern, Switzerland*
[d] *University of Bern, Department of Chemistry and Biochemistry, Freiestrasse 3, 3012 Bern, Switzerland*
[e] *University of Bern, Oeschger Centre for Climate Change, 3012 Bern, Switzerland*

ARTICLE INFO

Keywords:
Uranium
Swiss Molasse
Swiss Plateau
Peat
Leaching

ABSTRACT

Increased uranium (U) concentrations are found in certain ground and surface waters of the Swiss Plateau. Analysis of more than 100 public fountains revealed that increased ^{238}U concentrations frequently occur close to the interface between the Lower Freshwater Molasse and the Upper Marine Molasse, cropping out in the western part of the Swiss Molasse Basin. Out of these locations, Mont Vully, situated ca. 20 km west of Berne, was studied in detail. As this hill consists of the two aforementioned stratigraphic Molasse units, it represents an ideal case study. Two springs at the northern slopes of Mont Vully exhibit the highest ^{238}U concentrations with more than 300 mBq/L and were thus monitored for almost two years in order to screen possible seasonal variations. Further water samples were collected from spring captures, creeks and drainage pipes. The pipes drain the farmland north of Mont Vully showing ^{238}U concentrations with more than 600 mBq/L. In order to discover the reason for the duplication in concentration, gamma dose rate measurements were accomplished on the farmland, revealing elevated dose rates of up to 160 nSv/h. These are located above ancient pathways of creeks that originated from Mont Vully. At these locations with elevated dose rates, three shallow sediment drill cores were taken and analyzed for their U content. The sediment cores can essentially be divided into three parts: (i) an upper soil with common U concentrations of about 30 Bq/kg ^{238}U, (ii) an U-rich peat horizon with concentrations of up to 500 Bq/kg ^{238}U, and (iii) an impermeable clay unit that acts as an aquitard with again minor ^{238}U concentrations. Radiocarbon dating of the U-rich peat horizon reveals ages younger than 8.1 kyrs. This study suggests that a wetland was formed on top of the impermeable clay layer after the last glaciation during the Holocene. The stream waters with ^{238}U concentrations of more than 300 mBq/L originating from Mont Vully contributed significantly to the water supply for the development of the wetland. Due to the reducing conditions that are present in wetlands, the dissolved U in the incoming streams was reduced and adsorbed onto organic matter. Accordingly, an entrapment for U was generated, persisting for at least 6 kyrs – a sufficient time to accumulate up to 500 Bq/kg. In the course of the last century, numerous wetlands in Switzerland were drained by capturing streams and installing drainage pipes to make the land suitable for agriculture. This kind of melioration was also done at the wetlands north of Mont Vully resulting in a subsequent change in redox conditions within the soil. The solubility of U depends on its oxidation state and U can be oxidized by oxygen-rich rainwater. The rainwater leached the U adsorbed on the peat yielding ^{238}U concentrations of more than 600 mBq/L. Consequently, the duplication of ^{238}U concentrations in the drainage water as compared to the original concentration that creeks brought into the ancient wetlands has been clarified during this study. Twenty of the analyzed public fountains in the Swiss Plateau exhibited a ^{238}U concentration of more than 50 mBq/L. All of them could have contributed to the formation of a wetland after the last glaciation, which leads to the assumption that the situation at Mont Vully is not a singularity in the Swiss Plateau.

---

* Corresponding author. Paul Scherrer Institute, Department for Radiation Safety and Security, 5232 Villigen PSI, Switzerland.
E-mail address: anja.pregler@psi.ch (A. Pregler).

[1] Deceased.

https://doi.org/10.1016/j.jenvrad.2019.106026
Received 3 June 2019; Received in revised form 9 August 2019; Accepted 10 August 2019

1. Introduction

Uranium (U) is a toxic heavy metal that is present in most of the Earth's crust with an average abundance of 1.8 ppm (Mason and Moore, 1982). It occurs in the form of three natural radioisotopes: ^{238}U, ^{235}U and ^{234}U with isotopic ratios of 99.27%, 0.72% and 0.0054%, respectively (Meija et al., 2016). U has four different oxidation states, U(III), U (IV), U(V) and U(VI). U(IV) and U(VI), with their corresponding oxides UO_2 and UO_3, are the most common ones. UO_2, which is barely soluble and occurs in hydroxides, phosphates and fluorites (Keith et al., 2015), is the predominant species in reducing environments. Under oxidizing conditions, as encountered in surface and shallow groundwater, U(IV) is oxidized to U(VI), forming the easily soluble uranyl cation UO_2^{2+}, which forms different complexes with carbonates, sulphate ions and organic ligands (Chabaux et al., 2008). Due to the long half-life of ^{238}U ($T_{1/2} = 4.45*10^9$ years) and its heavy atomic mass of 238.05 g/mol, the specific activity of ^{238}U is rather low with 12 kBq/g (L'Annunziata, 2012). The radiotoxicity of U only plays a minor role compared to its more serious chemical toxicity (EFSA, 2009). Since U exposure to the general public predominantly occurs by ingestion via food and drinking water, it can cause critical damage to the human body, especially the kidneys (ATSDR, 2013). Consequently, the World Health Organization (WHO) recommends a limit of 30 μg/L U in drinking water (WHO, 2011). In 2017, the Swiss Federal Department of Home Affairs introduced its limit for U in drinking water to 30 μg/L as well (EDI, 2017). This critical value equals 372 mBq/L ^{238}U in terms of activity concentration. The dimension of ingesting U by liquid food depends strongly on diverse factors, e.g. environment of the catchment area or even personal consumption behavior. Already in 1930, Sale (1930) conducted a first survey on salts and radioactive nuclides in mineral water. Since then, studies were regularly performed all over the world in order to quantify concentrations of naturally occurring radioactivity in drinking and groundwater (Baertschi and Keil, 1992; Bajwa et al., 2017; Baradács et al., 2001; Birke et al., 2010; Cothern and Lappenbusch, 1983; Godoy and Godoy, 2006; Shin et al., 2016; Vesterbacka, 2007; Walsh et al., 2014; Wu et al., 2014). All of these studies demonstrate increased radionuclide concentrations in drinking water, but the reason for it is usually not specified in detail. A comprehensive survey for Switzerland was presented by Stalder et al. (2012) who analyzed more than 5500 water samples from most cantons of Switzerland to illustrate the geographical distribution of U concentrations in drinking water. The published map shows increased U levels along the alpine arc where crystalline bedrock with naturally enhanced U concentration in minerals is common. The map interestingly highlights another area in the western part of the Swiss Plateau, where elevated U contents cannot simply be explained by an underlying crystalline basement. Some cantons of particular interest, e.g. the Canton of Berne, were not covered in the study of Stalder et al. (2012). These data gaps and the fact that the U source in the Swiss Plateau remains rather unclear, represent the main motivation for the present study. U in groundwater, together with Radon (Rn), usually occurs as major fraction within the group of natural radionuclides. But other elements like Radium (Ra) or Polonium (Po), even in lower concentrations, contribute as well to the dose rate. Therefore, certain daughter isotopes of the ^{238}U decay chain such as ^{226}Ra, ^{222}Rn, ^{210}Pb and ^{210}Po were also determined. Since naturally occurring radioactive isotopes rarely display an equilibrium state in water (Osmond et al., 1983), the relations between the individual isotopes were examined during the study. However, groundwater is not the only hydrological unit susceptible to elevated U concentrations. Werthmüller et al. (2015) found extraordinarily high U concentrations in drainage pipes under an agriculturally used area ending up in the Lyssbach creek (10 km northwest of Berne, Switzerland). The reason for these elevated concentrations in the surface water is an U accumulation in peat ca. 0.5 m below the soil surface that is constantly leached by rainwater. One reason that was considered as U source has been the occurrence of Allalin gabbro in the area around the Lyssbach. This material which commonly contains U ores can be found in the Swiss Plateau due to glacial transportation from the Alps. Another possible explanation are coal beds with enhanced gamma dose rates that can also be found close the Lyssbach area. However, the actual origin of the U accumulation at the Lyssbach area remains unclear. Several authors assumed phosphate fertilizers containing natural U to be responsible for similar accumulations but could not definitely prove this theory (Barisic et al., 1992; Bigalke et al., 2018; Liesch et al., 2015). Another general explanation is the uptake of diverse metals and trace elements that can occur in wetlands as described, amongst others, by Banning et al. (2013); Gonzalez et al. (2006); Krachler and Shotyk (2004); Li et al. (2015); Li et al. (2014); Schumann et al. (2017). This would indeed explain the process of accumulation but again does not clarify the origin of U in peat found in the Swiss Plateau. Consequently, the overall goal of this study was to explain the correlation between increased U concentrations in groundwater appearing at the slopes of Mont Vully and the U accumulation that occur underground of the farmland in the north of it. Another objective was to verify the origin of the increased U concentrations in groundwaters that can be found in wide parts of the Swiss Plateau.

2. Study area: Swiss Plateau

2.1. Geological outline

The Swiss Plateau geologically belongs to the tertiary Molasse basin, which traverses Switzerland on approximately 300 km between Lake Geneva in the SW and Lake Constance in the NE (Fig. 1). The basin is bordered to the SE by the Alps and to the NW by the folded Jura Mountains and has mostly a hillocked morphology. The development of the Swiss Plateau started in the Oligocene when the Alpine orogeny caused the formation of a foreland basin that was successively filled with sediments (Pfiffner, 2014). Although the sedimentary infill is heterogeneous, Studer (1853) classified the Oligocene and Miocene sediments of the Swiss Molasse into four groups: (i) Lower Marine Molasse (UMM); (ii) Lower Freshwater Molasse (USM); (iii) Upper Marine Molasse (OMM) and (iv) Upper Freshwater Molasse (OSM), for which the conventional German abbreviations (brackets) are used in this paper. The four groups themselves are classified into two lithostratigraphic megasequences, UMM/USM and OMM/OSM. Both megasequences display the change from a marine to a continental environment, each one coarsening, thickening and shallowing upward (Sinclair et al., 1991). Of particular interest for the present study is the transition between the two megasequences, i.e. the interface between USM and OMM. In the middle of the Oligocene, freshwater lakes started to become shallower ending up in a dry area that are now the sediments of the USM. During this process, dying organic material accumulated on large conglomerate and sandy alluvial fans (Matter et al., 1980) leading to reducing conditions in shallow water. Consequently, dissolved U species in water originating from granitic and metamorphic clasts precipitated as UO_2 (uraninite) owing to the anoxic environment at the latest stage of the USM in mainly clayey to marly sediments (Cumberland et al., 2016; Matter et al., 1980). The transgression of the Burdigalian Sea in Miocene buried the deposited UO_2 under glauconitic marine sandstones, leaving behind an interface between USM and OMM partially loaded with U-rich fossils (Schott and Wiegand, 2003). According to Keller (1992), the UMM, USM and OSM act as aquitards with some sporadic water-bearing layers, whereas the OMM represents the only aquifer in the Molasse sequence. In the Pleistocene, the ice of the Würm glaciation locally eroded the OSM, leading to an exhumation of the OMM aquifer that now crops out as the uppermost unit in certain areas (Ramseyer, 1952).

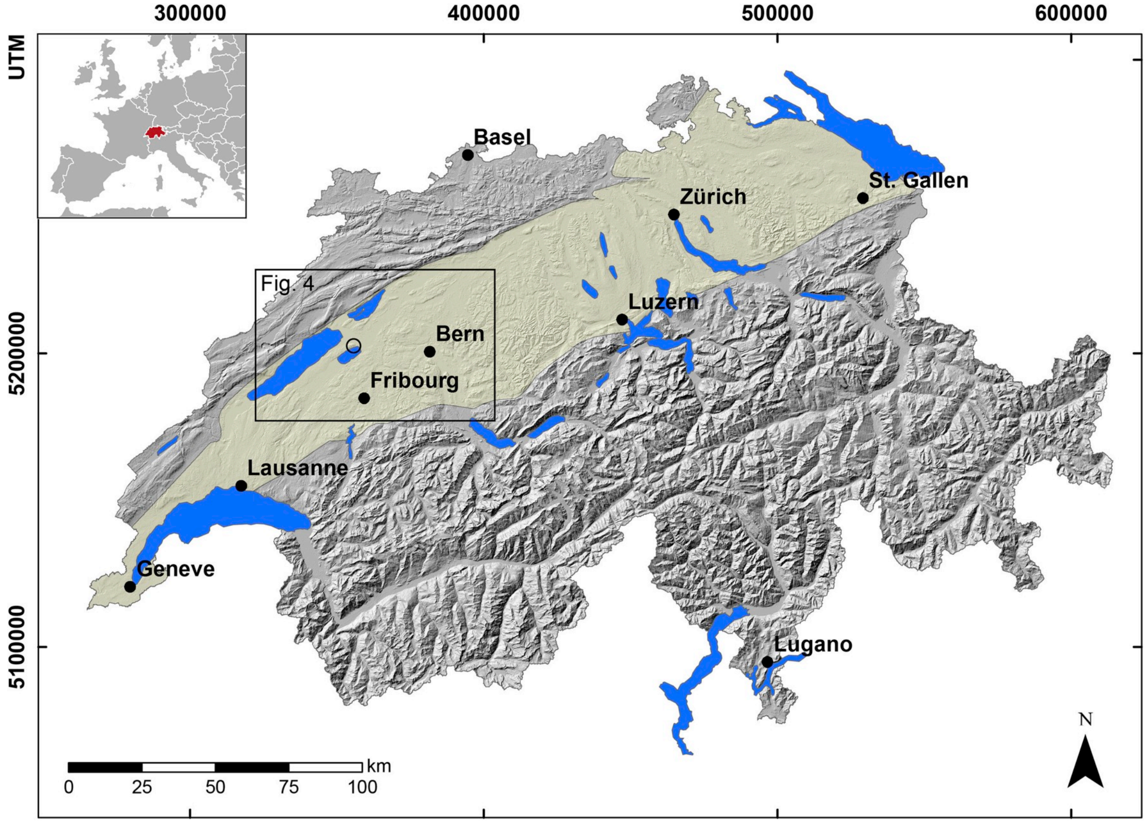

Fig. 1. Shaded relief map of Switzerland indicating the dimension of the Swiss Plateau (yellow), the area of the broader sampling campaign (rectangle) and the location of the intensively studied site Mont Vully (circle).

2.2. Case study Mont Vully

Mont Vully, located ca. 25 km west of Berne, was chosen as our main study site to investigate the relationship between increased U concentration in groundwater and accumulated U in soils of the Swiss Plateau (Fig. 1). The site comprises the hill of Mont Vully itself and the adjacent farmlands to the north (Fig. 2). Mont Vully has a height of 653 m a.s.l (the elevation of the surrounding plateau is 430 m a.s.l) and is composed of an USM-OMM sequence (Fig. 3a). Its detailed geology has been extensively studied earlier (Antenen, 1936; Becker, 1973; Ramseyer, 1952; Schott and Wiegand, 2003). Of particular importance for this study is that rainwater infiltrates the OMM aquifer until it is dammed by the impermeable USM. The convex interface between the USM and OMM at Mont Vully acts as a reservoir for the incoming rainwater and consequently leads to the occurrence of several springs at the slopes of the hill (Ramseyer, 1952). The discharged water accumulates to small creeks that have been existing since the last glaciation (Becker, 1973). The continuous supply of water in combination with an underground impermeable layer led to the formation of wetlands north of Mont Vully. At the beginning of the 19th century, numerous wetlands in Switzerland were drained in order to create arable land for agriculture (Graf et al., 2007). Commonly, this was accomplished by perforation of the impermeable layers and installation of drainage pipes that allowed runoff of the excess water to leave a dried peat layer underground behind. In the case of Mont Vully, there are two drainage pipes that feed the Broye Canal north of the hill (Fig. 2). Most of the springs that formerly fed the wetlands are nowadays captured for water supply and only some little creeks are left. Changes in the flow paths of the creeks can be traced in the "Journey through time – maps" provided by the Swiss Federal Office of Topography (2019b).

3. Material and methods

3.1. Collection of water samples

In the course of this study, 103 water samples were taken from a broad area in the Swiss Plateau, concentrated along the USM/OMM interface (Fig. 4) in order to map increased U concentrations. Most of the sampling points are public fountains. Formerly used as drinking troughs for farm animals, they can be found in the majority of old parts of towns and villages in Switzerland. The fountains are usually fed by sources from the close vicinity and are not treated by the local water supply facilities. The sampling campaign was accomplished in October 2017 as well as in July, October and December 2018. For each sampling site, one 250 mL polyethylene bottle was completely filled with water and subsequently acidified with a few drops of concentrated nitric acid (HNO_3) to prevent adsorption of radionuclides onto the bottle walls. Filtration was not necessary since there was no suspended matter visible. However, it was tested for several samples and the results in the filtered and unfiltered aliquots were identical within uncertainties. Only U isotopes were analyzed in these water samples.

At Mont Vully, the following sites were sampled for radionuclide analysis (Fig. 2): (i) 3 creeks, of which one was sampled at two locations: at the top and at the foot of Mont Vully, (ii) 6 sealed spring captures that are only accessible with the permission of authorities, (iii) 2 drainage pipes that are installed under the farmland north of Mont Vully and (iv) 2 public fountains. The two public fountains (No. 1: Fontaine Marylène in the west and No. 2: Fontaine du Stand in the north of Mont Vully) were continuously sampled in a monthly interval for two consecutive years in order to screen possible seasonal variations. A complete radionuclide analysis of ^{238}U, ^{234}U, ^{226}Ra, ^{222}Rn,

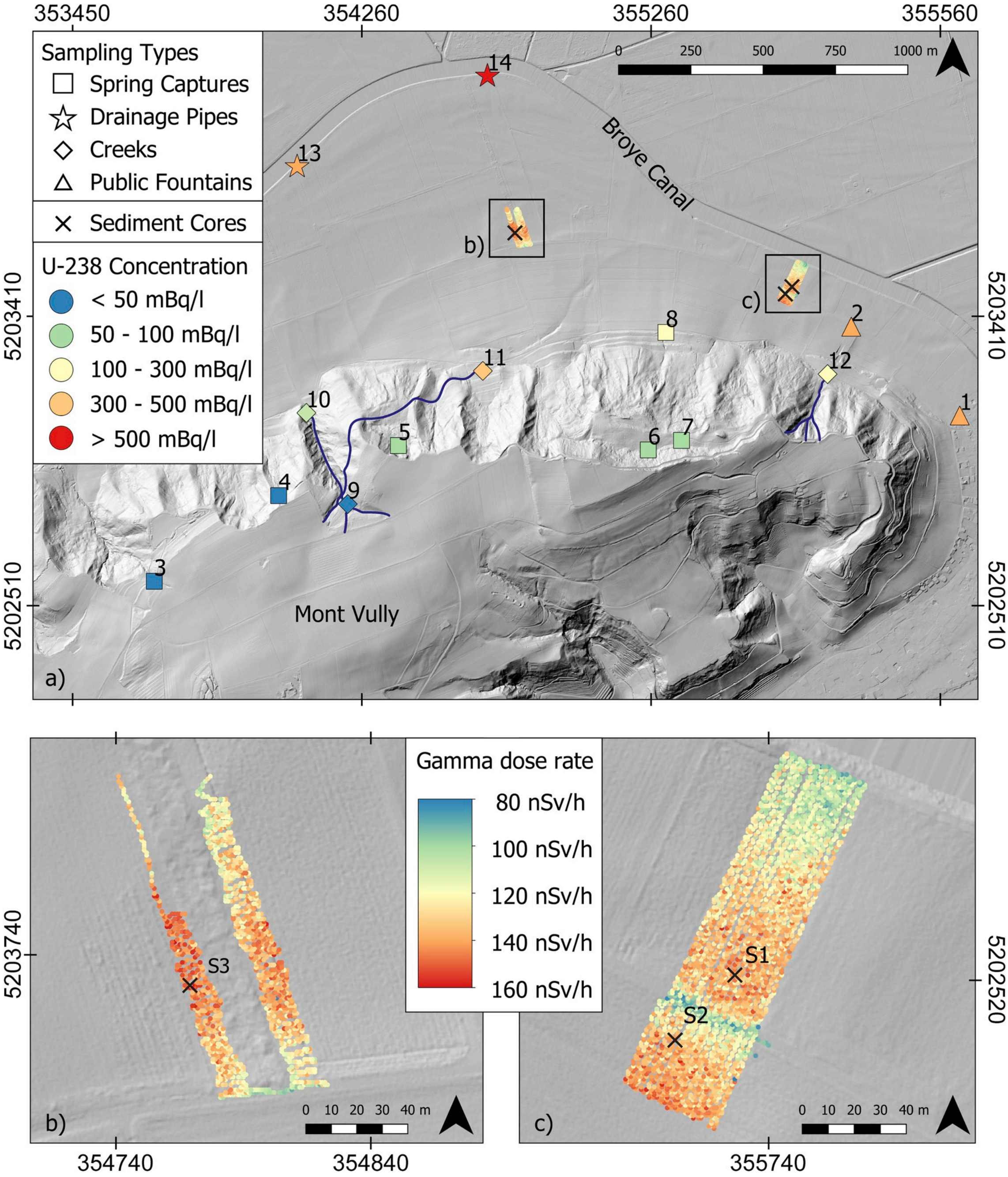

Fig. 2. Shaded relief map of the study site Mont Vully (Source of lidar data: GIS Competence Centre, Department of Land-Registry and Geomatics, Canton Fribourg). a) Four different water sampling types at Mont Vully indicating the ^{238}U concentration of each water sample. Numbers 1-14 correspond to the numbers listed in table 1. Crosses show the location of the 3 sediment cores. b + c) Detailed map of the gamma dose rate measurements north of Mont Vully showing the exact location of the sediment cores in related to the dose rate.

^{210}Pb and ^{210}Po was accomplished for these samples. Two 1L polyethylene bottles were completely filled and acidified with a few drops of concentrated HNO_3. For the ^{222}Rn measurements, special 20 mL glass vials with a gas tight septum in the cap were used in order to preclude the gaseous Rn to degas out of the water. The vials were overfilled and carefully closed in such a way that no air bubbles remained inside the vial. For the public fountains, electrical conductivity, pH and temperature of the outflowing water were immediately determined in the field using a handheld meter (HI98129 COMBO Tester from HANNA Instruments Switzerland AG). Furthermore, the flow rates of the two springs were measured in order to evaluate the radionuclide concentration after subsequent laboratory analyses. Only 250 mL were needed for the remaining 12 sampling locations at Mont Vully (No. 3–14) since they were simply analyzed for their U content.

3.2. *Laboratory water sample analysis*

3.2.1. *Determination of ^{238}U and ^{234}U*

For the analysis of two of the three naturally occurring U isotopes, 250 mL of the water sample were acidified with 5 mL concentrated HNO_3 and evaporated to complete dryness. Chemical yield was checked by adding ^{232}U as radiotracer. The residue was re-dissolved, filtrated

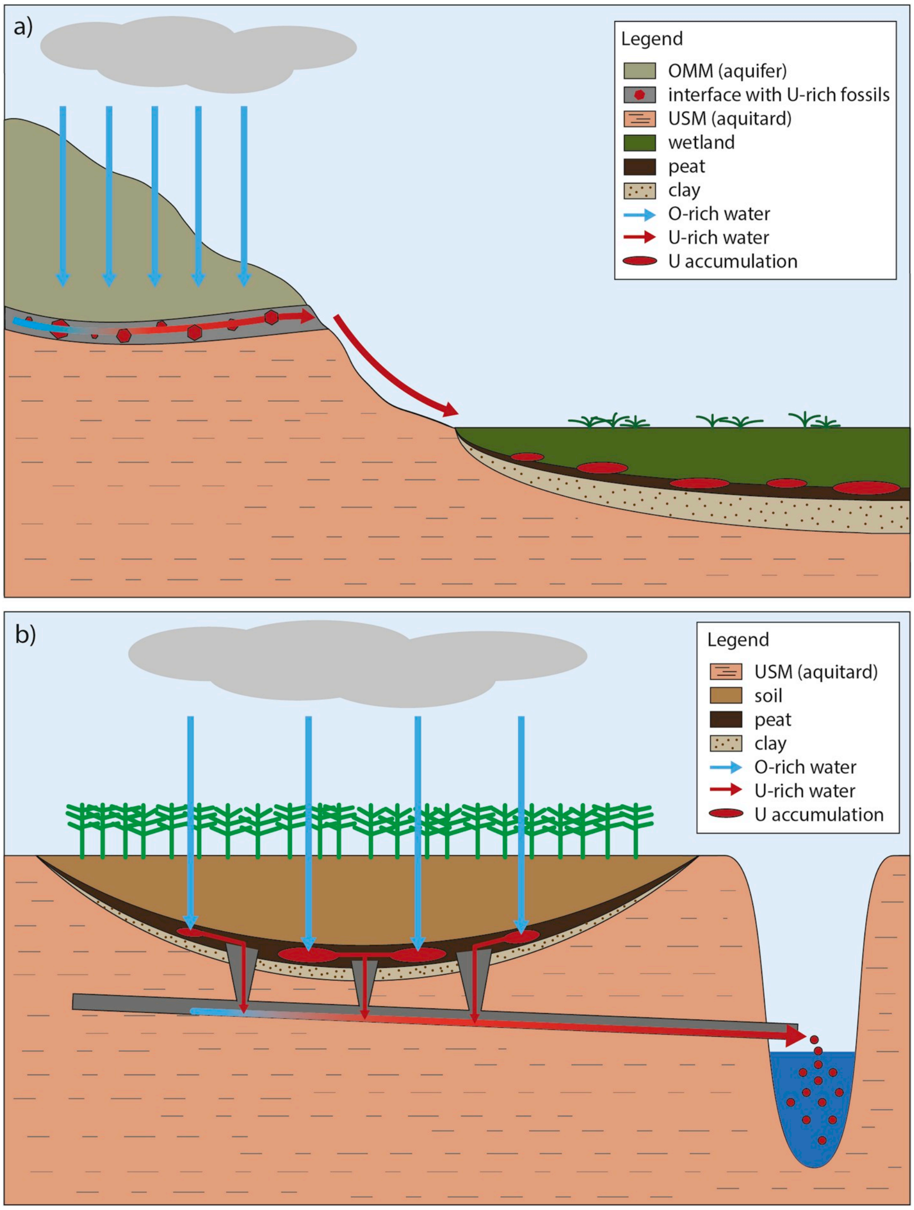

Fig. 3. Schematically drawn cross-section illustrating different stratigraphic units at Mont Vully and the farmland north of it. Not drawn to scale. a) Oxygen-rich rainwater infiltrates OMM, leaches U adsorbed onto fossils and becomes U-rich groundwater that accumulates in the reducing environment of the developing wetland. b) Oxygen-rich rainwater infiltrates drained wetland and leaches accumulated U in a peat horizon before ending up in surface waters.

through a 0.45 μm cellulose nalgene filter and passed through a Triskem U/TEVA column to separate U from Ra, Po and Th. The procedure of the chromatographic extraction was adapted from the procedure of Horwitz et al. (1992). The resulting concentrated U solution was used for electrodeposition onto a stainless steel disk. The detailed electrodeposition procedure is described in Bajo and Eikenberg (1999). The disk was measured using an Octête PC α-spectrometer from ORTEC.

3.2.2. Determination of ^{210}Po

The activity concentration of ^{210}Po was determined by spontaneous adsorption of Po onto a silver disk. The chemical yield of the adsorption process was controlled by adding a defined amount of ^{209}Po tracer. The water sample was acidified with concentrated HCl. Ascorbic acid was added to reduce potential Fe(III) to Fe(II). A silver disk with 28 mm in diameter was mounted into a Teflon holder in that way, that only one side of the silver disk was in contact with the solution. The holder was completely placed into the solution for approximately 24 h under continuous stirring. After adsorption, the disk was directly measured by α-spectrometry for one week. The procedure was adapted from Lee et al. (2014).

3.2.3. Determination of ^{226}Ra and ^{210}Pb

^{226}Ra was analyzed together with ^{210}Pb by means of a 3M Empore Rad Disk filter. The procedure was adapted from Wallner et al. (2008). Since activity concentrations were expected to be extremely low, 1.5 L of sample volume was needed to reach an appropriate detection limit of 50 mBq/L. Pb was extracted from the Rad Disk filter with 5 mL di-Ammonium hydrogen citrate (DHC) and mixed with 15 mL Optiphase Hisafe 3 scintillation cocktail from PerkinElmer. Ra was eluted with 5 mL alkaline EDTA solution and mixed with 15 mL Goldstar scintillation cocktail from Meridian. Liquid scintillation counting was performed using an HIDEX 300 SL scintillation counter with simultaneous α/β-counting and pulse shape analysis. A detailed explanation of this counting method is given in (Eikenberg et al., 2014).

3.2.4. Determination of ^{222}Rn

Radon was also analyzed by means of liquid scintillation counting. With the help of a syringe, 5 mL of the immiscible liquid scintillation cocktail MaxiLight from HIDEX were carefully sublayered with 10 mL of sample water in a 20 mL scintillation vial. After vigorously shaking the vial, ^{222}Rn and its short-lived daughters are equilibrated during 3 h and measured with a HIDEX 300 SL for 1 h with α/β-separation.

3.3. Gamma dose rate measurements

In order to discover potential U accumulations below the recent farmland at Mont Vully, gamma dose rate measurements were conducted either with a handheld 2″x2″ NaI(Tl) detector (a modified Gate Frisker from Ludlum) or with a large plastic scintillator (BDKG-32 from Atomex). These measurements were accomplished by walking grid-wise along the farmland, carrying the detector together with a GPS 1 m above ground. The count rate for the energy region from about 100 to 1000 keV was converted to approximate dose rates by calibration with an Automess 6150 AD-6/H connected to a large plastic scintillator 6150 AD-b/H. The detector records the total gamma radiation, which mainly originates from the decay products of ^{226}Ra such as ^{214}Pb or ^{214}Bi and quantifies the measurements with a sensitivity of 1 cps per nSv/h. Since these dose rate measurements a not precise enough, the results cannot be used for absolute quantification of U concentration in the underground, but they give an indication where U accumulations occur in the soil. Due to the fact that the area north of Mont Vully is intensively used for agriculture, the dose rate measurements were restricted to two small fields where it was possible to walk without destroying any crops (Fig. 2). On the basis of these measurements, locations with elevated dose rates were selected for soil sampling.

3.4. Soil sampling and analysis

In March 2018, three sediment cores (S1 – S3) were drilled into 1 m depth at the previously identified locations north of Mont Vully by means of vibrocoring with the portable drilling unit "Cobra" of Atlas Copco (Fig. 2). The cores with an inner diameter of 6 cm were cut into 5–10 cm pieces and packed into plastic bags for protection. In the laboratory, the samples were unpacked, dried in the oven at 105 °C for 15 h and ground to a homogeneous powder. An aliquot of each sample was wet and dry ashed and leached by boiling the residue in 8 M HNO_3 and 30% H_2O_2 for 1 h. The suspension is filtrated to separate the leached fraction from insoluble compounds. Afterwards, U was analyzed identically to the procedure already used for the water samples (section 3.2.1).

3.5. ^{14}C dating

Dating of the peat horizons from the sediment cores was accomplished by the ^{14}C method. Potential fractions of carbonate and humic acids were removed from an aliquot of the samples using an acid-base-acid treatment. Subsequently, the residue was completely combusted and then transformed into graphite targets. Measurements were conducted with the accelerator mass spectrometer (AMS) MICADAS at the LARA laboratory at the University of Bern. The detailed procedure is given in Szidat et al. (2014). The measured ^{14}C ages were calibrated using IntCal13 to provide the calendar ages of the samples (Reimer et al., 2013). The lower and the upper part of the peat horizons from the drilling cores of the former wetland were used for dating in order to estimate the beginning and the end of the peat deposition period and to verify if the sediment cores still show an undisturbed sequence at least below the tillage depth. For the first sediment core (S1), two peat horizons extend from 45 to 60 cm depth and from 80 to 90 cm depth, while one peat horizon is located each in sediment core 2 (S2) and sediment core 3 (S3) in 75–100 cm and 65–100 cm depth, respectively.

4. Results

4.1. Extended sampling campaign in the Swiss Plateau

The U concentrations in water samples of the extended sampling campaign range from 4 ± 2 mBq/L for ^{238}U and 5 ± 3 mBq/L for ^{234}U to 239 ± 35 mBq/L for ^{238}U and 298 ± 43 mBq/L for ^{234}U (Fig. 4). Twenty of the 103 samples display a ^{238}U activity concentration of more than 50 mBq/L and 10 of more than 100 mBq/L. Due to the protection of data privacy, the exact values and locations of the extended sampling campaign are not specified. The highest value in the here studied part of the Swiss Plateau was found for one sampling date

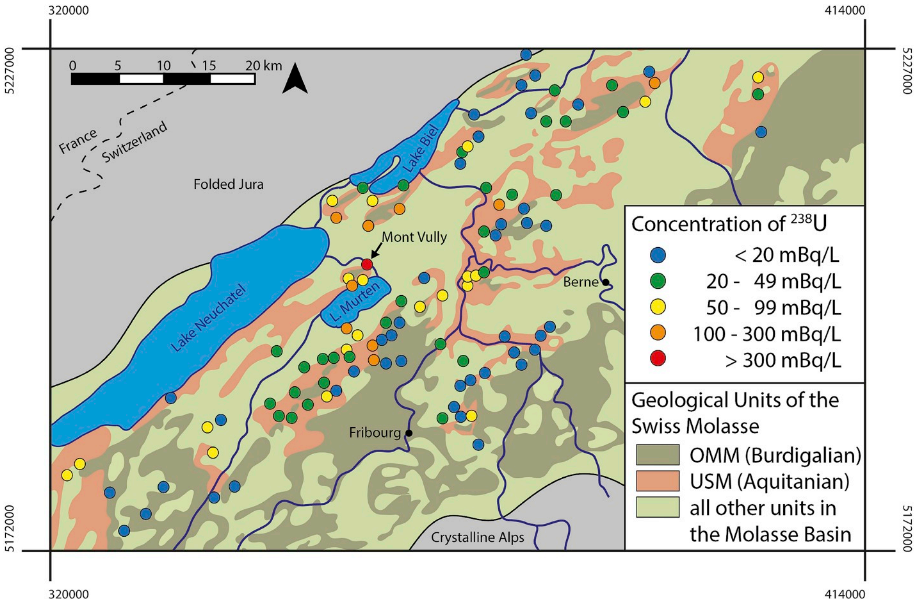

Fig. 4. Geological map of the Molasse basin indicating the areas where USM (pink) and OMM (brownish) are outcropping. Colour-coded dots show the water sampling locations with their according U activity concentrations.

at Mont Vully with 395 mBq/L ^{238}U. This was the only sampling location that exceeded the Swiss EDI limit for U of 30 μg/L, which corresponds to 375 mBq/L ^{238}U.

4.2. U-series disequilibrium in water at Mont Vully

The two public fountains at Mont Vully were continuously monitored once per month over a two-year period from 2016 to 2018, allowing for a detection of seasonal effects. The sampling campaign for Fontaine Marylène (No. 1) started in June 2016 with a total of 20 water samples; sampling of Fontaine du Stand (No. 2) was initiated in November 2016 with a total of 17 water samples. For these two sampling points at Mont Vully, the flow rate depended upon the amount of precipitation in the catchment area. The monthly and annual precipitation can be tracked at the corresponding maps of MeteoSwiss, which show that a dry period leads to a lower flow rate approximately 6 months afterwards (Federal Office of Meteorology and Climatology MeteoSwiss, 2019). For both springs, the water temperature was directly coupled with the seasonal outside air temperatures: highest water temperatures were found in September 2017 with 20 °C; lowest in January 2017 with 5 °C. The pH of 7.4 ± 0.1 as well as the electric conductivity of 610 ± 15 μS/cm were constant throughout the whole

Table 1
^{234}U and ^{238}U concentrations and AR in different water samples at Mont Vully. The numbers in the first column correspond to the numbers in Fig. 2.

No. in Fig. 2	Type	^{238}U [mBq/L]	±	^{234}U [mBq/L]	±	AR
1	public fountain (mean value)	319	26	346	25	1.1
2	public fountain (mean value)	308	22	333	18	1.1
3	spring capture	36	7	31	7	0.8
4	spring capture	32	7	28	7	0.9
5	spring capture	82	18	88	18	1.1
6	spring capture	86	15	75	14	0.9
7	spring capture	100	17	88	16	0.9
8	spring capture	290	30	301	30	1.0
9	creek	37	8	39	8	1.0
10	creek	60	11	65	12	1.1
11	creek	361	56	327	51	0.9
12	creek	204	23	193	22	0.9
13	drainage pipe	402	58	361	53	1.1
14	drainage pipe	626	88	648	90	1.0

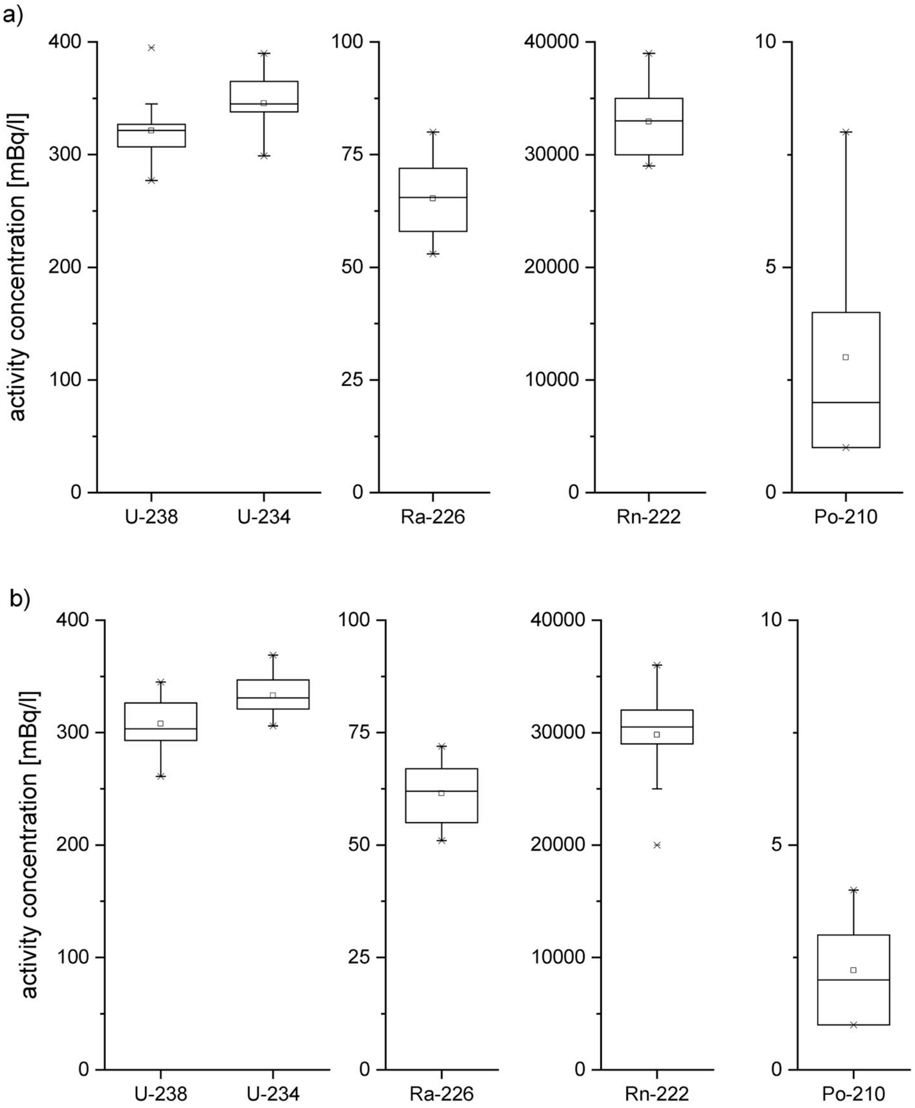

Fig. 5. Boxplot diagrams of a) Fontaine Marylène and b) Fontaine du Stand indicating the activity concentrations for the different radioisotopes of the ^{238}U decay series throughout the whole sampling campaign. Note the different scales of axes.

sampling campaign. The activity concentrations exhibit a complete disequilibrium within the ^{238}U decay series, but the concentrations within one particular isotope in the decay chain are fairly constant (Fig. 5). The highest values were found for ^{222}Rn with a mean of 32000 ± 4000 mBq/L and 31000 ± 3000 mBq/L for Fontaine Marylène and Fontaine du Stand, respectively. Lowest concentrations were found for ^{210}Po with 3 ± 2 mBq/L for Fontaine Marylène and 2 ± 1 mBq/L for Fontaine du Stand. ^{210}Pb activity concentration for all samples were below the detection limit of 50 mBq/L. But due to the rather short half-life of ^{210}Po ($T_{1/2}$ = 138 days), ^{210}Pb and ^{210}Po should be in secular equilibrium and the activity concentration of ^{210}Pb can be expected to be in the same range as ^{210}Po. A mean of 62 ± 8 mBq/L for both springs was detected for ^{226}Ra. The activity concentrations of the two U isotopes lie within the same range for both fountains: Fontaine Marylène exhibited mean values of 319 ± 26 mBq/L and 346 ± 25 mBq/L for ^{238}U and ^{234}U, respectively, and Fontaine du Stand displayed mean values of 308 ± 22 mBq/L and 333 ± 18 mBq/L for ^{238}U and ^{234}U. The activity ratio (AR) of ^{234}U/^{238}U was equal with 1.08 ± 0.04 for both fountains. All activity concentrations were constant within uncertainties over the whole sampling period, regardless of seasonal variations like temperature or precipitation. The results of the U analysis for all sampling locations at Mont Vully are listed in Table 1.

4.3. Gamma dose rates at Mont Vully

Gamma dose rate measurements on the farmland north of Mont Vully revealed increased gamma dose rates of up to 160 nSv/h including background radiation. In other parts of the area north of Mont Vully, only 80 nSv/h was detected (Fig. 2). The locations with elevated dose rates were selected as sites for percussion drilling, since they offer the highest probability of finding an U accumulation.

4.4. Uranium content of soil samples

All three sediment cores can essentially be divided into three parts: (i) an upper part that consists of soil and loam with common U concentrations of about 30 Bq/kg ^{238}U, (ii) an U-rich peat horizon with concentrations of more than 500 Bq/kg ^{238}U, and (iii) an impermeable clay unit that acts as an aquitard with again minor ^{238}U concentrations (Fig. 6). However, the sediment cores differed from each other in their total U content as well as in the depth where the U-rich peat horizons were located. S1 exhibited the highest ^{238}U concentrations of all sediment cores at a depth of 55–60 cm with 543 ± 75 Bq/kg. S2, which was taken only 45 m away from S1, showed values of 313 ± 36 Bq/kg ^{238}U at 95–100 cm depth. The highest concentrations in S3 were found at 90–100 cm depth with an activity concentration of 437 ± 49 Bq/kg ^{238}U. The ^{234}U/^{238}U AR in all peat samples was 1.06 ± 0.03.

4.5. ^{14}C ages of peat at Mont Vully

Radiocarbon dating of the peat yielded slightly different ages for all three sediment cores. The lower part of the first peat horizon of S1 in 55–60 cm depth was dated to 3765 ± 20 years, the upper part at 40–45 cm depth to 1875 ± 20 years. The second peat horizon of S1, that extends from 80 to 90 cm depth, was dated to 7180 ± 25 years at the lower end. S2 revealed similar ages of 3415 ± 20 years and 1815 ± 20 years for the lower (95–100 cm) and upper (75–80 cm) part of the peat horizon, respectively. S3 showed higher ages of 5230 ± 20 years at 90–100 cm depth and 2765 ± 20 years at 60–70 cm depth. From these ^{14}C ages, the following calibrated age ranges of the peat horizons were deduced (Fig. 6): S1: 1.8–1.9 to 7.9–8.0 kyrs, S2: 1.8–1.9 to 3.6–3.8 kyrs, S3: 2.8–3.0 to 6.0–6.1 kyrs. As these calibrated age ranges only allow an estimation of the duration of the peat formation (see below in the Chapter Discussion), they are given in centennial resolution.

5. Discussion

In the following, we present our model for the increased U concentrations in soil, ground and drinking water in the Swiss Plateau as a four-stage process of U accumulation and leaching. The first two steps – originally suggested by Schott and Wiegand (2003) – comprise the accumulation of U at the USM/OMM interface in Oligocene and the ongoing leaching of U-rich fossils by infiltrating rainwater at this interface (Fig. 3a). The third and fourth step are findings of the present study and include the accumulation of U in bogs and wetlands and anew leaching processes that started in the 19th century, when wetlands were drained (Fig. 3b).

As already explained in section 2, fossils encrusted with U can be found at the interface between USM and OMM along the western part of the Swiss Plateau (Ramseyer, 1952). Since the USM represents an aquitard, rainwater with high oxygen content infiltrates the OMM and is retained at the interface between the two Molasse units where U-rich fossils occur (Fig. 3a). The study of Schott and Wiegand (2003) identified the following process: At the USM/OMM interface, the rainwater oxidizes the precipitated insoluble U(IV) to soluble U(VI) resulting in a constant leaching process of the fossils. The rainwater with dissolved U migrates along the impermeable USM until the interface reaches the surface. At these points, springs of groundwater with increased U activity concentrations are welling out of the hills. Extended sampling on the basis of geological maps accomplished by the present study highlights the frequency of enhanced U concentrations along the USM/OMM interface (Fig. 4). The characterization of the water samples that are in connection with the interface is based on the stratigraphy of the two Molasse units, i.e. the OMM (brownish in Fig. 4) lies above the USM

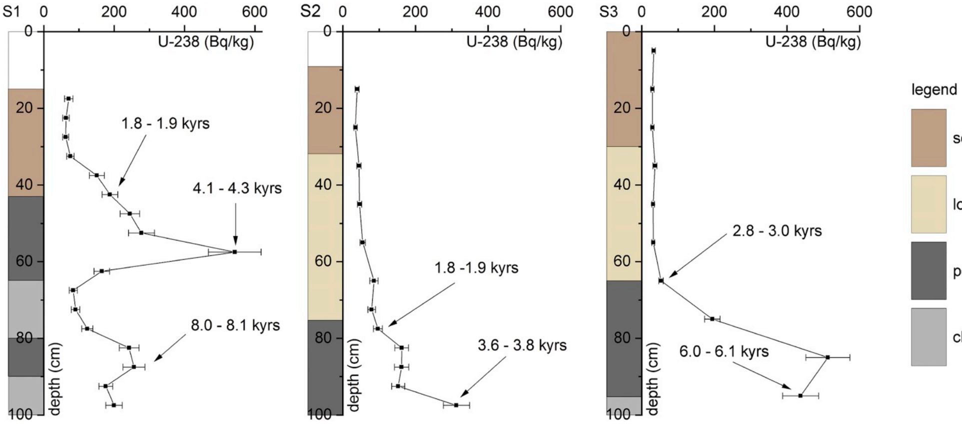

Fig. 6. ^{238}U concentration of the 3 sediment cores plotted against depth. Colour-coding at the left side of the Y-axis illustrates the different soil components of each sediment core. Additionally, the ^{14}C ages are labelled at the corresponding depth.

(pink in Fig. 4). For water samples that are located only in the OMM it is impossible to pass the interface and therefore cannot leach potential U accumulations. None of these samples in the OMM show increased U concentrations. Water samples that derive from an area where the interface could have been passed show moderate to increased U concentration. Certainly, there are water samples that are located at the interface and do not show increased concentrations. These samples either pass the interface at an area where there is no U accumulation or the interface is not passed at all in spite of its vicinity. This correlation can be seen more in detail at Mont Vully. The sample locations which derive only from the OMM on top of the hill (No. 3, 4 and 9 in Fig. 2) exhibit nearly no U content in comparison with the water samples that are located below the USM/OMM interface (No. 1, 2, 8, 11, 12 in Fig. 2). Waters sampled on the slopes between the top and bottom of Mont Vully show intermediate concentrations (No. 5, 6, 7, 10 in Fig. 2). The creek that was sampled at two locations is the best example in that regard: The ^{238}U concentration doubles in value from the very top (No. 9 in Fig. 2) of Mont Vully until the foot (No. 10 in Fig. 2). This implies that there is a groundwater flow with increased U concentration into the creek before it reaches the second sampling location. The two springs with water originating from the USM/OMM interface that were selected for a detailed investigation of U concentrations are Fontaine Marylène (No. 1 in Fig. 2) and Fontaine du Stand (No. 2 in Fig. 2). It is known from the municipal water supply responsible Mr. Biolley (personal communication, January 2017) that they originate from one source deriving from the U-rich interface but cover different distances until they reach the surface. For this reason, the two sources are considered as one in the following explanations. The fairly constant values throughout the whole sampling campaign (Fig. 5) demonstrate that the water of the fountains is rather groundwater that, in comparison with surface water, is not quickly prone to changes in geochemical conditions. As well as Schott and Wiegand (2003) we assume steady oxidizing conditions at the USM/OMM interface that allow U to be leached (Ivanovich and Harmon, 1992). Therefore, U occurs in increased activity concentrations in the water, whereas its decay products remain unleached. ^{226}Ra is rarely soluble under oxidizing conditions (Faure and Mensing, 2005) and is measured only in small amounts of maximum 80 mBq/L. The same is true for ^{210}Po, which is poorly soluble (Ivanovich and Harmon, 1992) and therefore does not even allow the detection limit to be reached in some of the water samples. However, speciation taking into account that radionuclides may not only be transported as dissolved ions or complexes but also attached to colloids (inorganic and organic matter, e.g. extracellular bacterial material (Larock et al., 1996; Ram et al., 2019)) was not covered in this work. Transport by colloids might explain the ^{210}Po values found in some of the water samples but further investigation needs to be done. The radionuclide that exhibits highest activity concentrations is ^{222}Rn with almost 40000 mBq/L. This is obvious since Rn is the only gaseous element in the ^{238}U decay chain and can be transferred into water much easier than solids. The mean AR of ^{234}U/^{238}U was 1.08 ± 0.04. The reason for these increased values of ^{234}U in comparison to ^{238}U in water is preferential leaching from the solid phase, enabled by radiation damage of the crystal lattice. This damage is the result of recoil that breaks the bond which retains the nuclide inside the crystal lattice resulting in a better leachability of the following isotopes in the decay chain (Osmond and Cowart, 1976). Consequently, the leached solid phase should exhibit depletion in ^{234}U.

The next part in this four-stage process is directly connected to the U-rich groundwater found in certain parts of the Swiss Plateau. After the end of the last glaciation and later during the Holocene, bogs and wetlands had developed on top of an impermeable clay layer north of Mont Vully due to the constant supply of water from the USM/OMM interface on the one hand, and a lack of possibilities to runoff on the other hand (Fig. 3a). Dying organic material and microbial degradation led to a reducing environment in the wetlands and cumulated organic matter was deposited in the peat horizon on top of the clay layer. The solubility of U is very sensitive to redox conditions. When dissolved U species in groundwater deriving from the USM/OMM interface enter the anoxic environment in the wetland, the soluble U(VI) is reduced to insoluble U(IV) and adsorbs onto organic material (Wang et al., 2014). Accumulation over thousands of years led to a considerable amount of U in the wetland peat, although the concentration of the input water was comparably small. Measurements of gamma dose rates on the farmland north of Mont Vully already indicate an accumulation of U in a peat horizon underground, as evidenced by gamma radiation that is highly increased with respect to normal background values. Rybach et al. (2002) reported an average total dose rate of 147 nSv/h in Switzerland combining artificial, cosmic and natural terrestrial dose rates. However, this value considers all parts of Switzerland including highly enhanced dose rates originating from the Alpine region with natural terrestrial dose rates that reach a maximum of 368 nSv/h (Rybach et al., 2002). Considering the average total dose rate in the area of Mont Vully, values above 80 nSv/h are clearly enhanced in comparison to the normal background (Rybach et al., 1997). As these values are no absolute values and vary with depth of the U-rich peat horizon, verification had to be done by analyzing the soil itself. The results of the cores confirm that the peat horizon has accumulated a considerable amount of up to 543 ± 75 Bq/kg ^{238}U (this value equals 43.8 ppm ^{238}U) in spite of the rather low U concentration of the incoming water with only approximately 350 mBq/L ^{238}U (this values equals 0.03 ppm ^{238}U) – assuming these concentrations were constant over the Holocene. Radiocarbon dating of the organic material at the lower end of the peat horizons revealed an onset of the peat formation of around 4–8 kyrs ago (Fig. 6). This verifies the assumption that the wetlands began to form after the Würm glaciation, when an excess of water was available. Sediment core S1 revealed, however, that there is more than one peat horizon, separated from each other by a 15 cm thick clay layer. This indicates that there have been several peat accumulation cycles, which were not covered by the soil cores into 1 m depth. It is very likely that there are more peat horizons below 1 m and that the real onset of peat formation started earlier. We therefore assume that the onset started at the earliest 16 kyrs ago when the Würm glaciation terminated (Ndiaye et al., 2014). The development of the uranium-accumulating peat in sediment core S1 started during the onset of the mid-Holocene summer maximum ~8 ky ago. The maximum U concentrations in all 3 sediment cores are in 4 kyrs old peat layers. This coincides almost with the highest level of the mid-Holocene summer maximum in Central Europe which was ~6 ky ago (Davis et al., 2003). According to the dating results, the end of peat accumulation seems to have occurred 2–3 kyrs ago. We assume, however, that peat formation discontinued only a few centuries ago after a land-use change from near-natural wetland to an intensively managed grassland. This change typically involves a decrease of the water table, which promotes aerobic decomposition of sub-surface peat so that the ^{14}C age of the top peat layer appears to be older than the date of the land-use change (Krüger et al., 2015). Since then, the former wetland was covered with a soil layer of up to 70 cm thickness. The upper soil was not infiltrated with U-rich groundwater and therefore does not show increased U values. The concentrations lie in the normal range for a common soil of around 30 Bq/kg ^{238}U due to its original mineral components. Dating the upper and lower part of the cores also confirms an undisturbed sequence of the sediments.

In the beginning of the 19th century, plenty of wetlands were drained in the Swiss Plateau in order to create arable land (Graf et al., 2007). This comprehensive melioration was accomplished on the one hand by capturing incoming streams to reduce water supply (Swiss Federal Office of Topography, 2019b) and on the other hand by perforating the impermeable clay layers to install drainage pipes beneath. These measures effected runoff of the retained water in the bog (Fig. 3b). Breaking up the soil combined with infiltrating oxygen-rich rainwater caused a change in redox conditions from anoxic to oxic. This led to an oxidation of U(IV) to U(VI), which is adsorbed onto soil particles and organic matter. Since then, continuously seeping rainwater resulted in an ongoing leaching process within the U accumulation in the soil. This process yields even higher U concentrations in the resulting drainage water (650 mBq/L ^{238}U of No. 13 in Fig. 2) than those that have been introduced into the ancient wetlands via the creeks (360 mBq/L ^{238}U of No. 11 in Fig. 2) during the accumulation period ~2–8 kyrs ago. All the activity concentrations in groundwater, surface water and water of the drainage pipes under the farmland north of Mont Vully as well as the results of the peat horizon reveal that the described processes are perfectly applicable to Mont Vully: The sampled water of the pipes is rainwater that percolated through the soil and peat horizons before ending up in the Broye canal. This whole process can be traced by the AR of three different stations: the water originating from (i) the USM/OMM interface, (ii) the peat itself and (iii) the drainage pipes. All of them exhibit an AR of 1.1. The initial AR of 1.1 that can be measured through the whole 2 years sampling period at the public fountains at Mont Vully is due to the preferential leaching of ^{234}U in comparison to ^{238}U. Once released from the mineral, ^{238}U and ^{234}U show the same chemical behavior. This means that the accumulation of U in the peat exhibits the same AR ratio of 1.1 as the incoming water since the adsorption processes onto the organic matter is chemically equal for all U isotopes. The same is true for the leaching processes from the peat into the drainage water where the AR again is 1.1. Although this track of AR is associated with some uncertainties, it nevertheless helps to illustrate the fate of U in the whole accumulation and leaching process.

Other U origins like phosphorous fertilizers can be excluded since the highest U concentrations occur at 50–100 cm depth while the upper top soil - where fertilizers are applied - does not show any increased values (Fig. 6). The results of the ^{14}C dating also controverts fertilizer as origin because the age of the horizons with highest U concentrations show ages of several thousand years. It is rather unlikely that the U accumulation took place only recently because decay products of ^{238}U such as ^{234}Th, ^{230}Th or ^{226}Ra were determined qualitatively. Due to inaccurate measurements, it was abandoned to publish the quantitative data. However, by considering the rough ingrowth of these ^{238}U daughters, the U accumulation must have started some thousand years ago. This verifies the assumption that the U accumulation and the peat formation happened simultaneously.

The presented study helps to clarify the situation at the Lyssbach creek where an U accumulation with unknown origin was found in a peat horizon (Werthmüller et al., 2015). Although there is currently no USM/OMM interface in the direct vicinity, it is still likely to be the origin since the OMM was only removed by erosion, leaving the USM behind. The two other possible reasons for the U accumulation that have been proposed by Werthmüller et al. (2015) have been considered to be unlikely. Both, the Allaline gabbro as well as the coal beds, can effectively result in increased U concentrations. However, Jouvet et al. (2017) elaborated a model to estimate the diversion of erratic boulders by the Valais glacier and came to the result that nearly no boulders were transported to the Solothurn lobe. The rareness of Allalin gabbro and coal beds in the Swiss Plateau can also be checked by consulting the corresponding geological maps (Swiss Federal Office of Topography, 2019a). This leads to the assumption that the frequency of Allalin gabbro occurrence is too low than having a high enough impact to lead to these increased concentrations.

As a final risk evaluation it has to be mentioned that most of the indicated U concentrations in ground and surface water are still below the Swiss regulatory guideline relating to drinking water (EDI, 2017). U concentrations in groundwaters of the studied part of the Swiss Plateau exceed the limit of 372 mBq/L ^{238}U only at one location at Mont Vully and this fountain is declared as no drinking water.

6. Conclusion

Increased U concentrations in groundwaters deriving from the USM/OMM interface have been confirmed by an extended sampling campaign in the Swiss Plateau. The origin of U accumulated in peat horizons is verified to originate from this interface. The whole process can be explained in the following four steps:

a) Adsorption of U onto fossils during the development of the USM/OMM interface.
b) Leaching of U by infiltration of O-rich rainwater into the OMM aquifer.
c) Accumulation of U in a peat horizon due to reducing conditions in wetlands.
d) Leaching of U after drainage of the wetland.

The situation and history at Mont Vully are applicable to other localities in the Swiss Plateau where (i) wetlands were drained and (ii) increased U concentrations are measured in groundwater near the USM/OMM interface. We therefore suggest further investigation of these sites.

Acknowledgements

The authors are very grateful to the local authorities and the farmers for their kind cooperation during sampling campaign, especially while soil sampling on the arable land. Further thanks go to Mr. Grandgirard from the GIS Competence Centre of the Canton of Fribourg for kindly providing the Lidar data of the area around Mont Vully. We acknowledge Dr. Martin Heule, Dr. Maya Jäggi (both PSI) and Peter Biermanns (RWTH Aachen, Germany) for the constructive and helpful comments to this work, and Irène Zumsteg and Dr. Andreas Brand (both PSI) for their assistance in the laboratories. This work was financially supported by the Swiss Federal Nuclear Safety Inspectorate (ENSI).

References

Antenen, F., 1936. Geologie des Seelandes. Verlag der Heimatkundekommision, Biel.

ATSDR, 2013. Toxicological Profile for Uranium.

Baertschi, P., Keil, R., 1992. Urangehalte von Oberflächen-, Quell- und Grundwässern der Schweiz. NAGRA, Wettingen.

Bajo, S., Eikenberg, J., 1999. Electrodeposition of actinides for α-spectrometry. J. Radioanal. Nucl. Chem. 242, 745–751.

Bajwa, B.S., Kumar, S., Singh, S., Sahoo, S.K., Tripathi, R.M., 2017. Uranium and other heavy toxic elements distribution in the drinking water samples of SW-Punjab, India. J. Rad. Res. Appl. Sci. 10, 13–19.

Banning, A., Demmel, T., Rüde, T.R., Wrobel, M., 2013. Groundwater uranium origin and fate control in a river valley aquifer. Environ. Sci. Technol. 47, 13941–13948.

Baradács, E., Hunyadi, I., Dezső, Z., Csige, I., Szerbin, P., 2001. ^{226}Ra in geothermal and bottled mineral waters of Hungary. Radiat. Meas. 34, 385–390.

Barisic, D., Lulic, S., Miletic, P., 1992. Radium and uranium in phosphate fertilizers and their impact on the radioactivity of waters. Water Res. 26, 607–611.

Becker, F., 1973. LK 1165 Murten Erläuterungen, Geologischer Atlas der Schweiz. Schweizerische Geologische Komision, Bern.

Bigalke, M., Schwab, L., Rehmus, A., Tondo, P., Flisch, M., 2018. Uranium in agricultural soils and drinking water wells on the Swiss Plateau. Environ. Pollut. 233, 943–951.

Birke, M., Rauch, U., Lorenz, H., Kringel, R., 2010. Distribution of uranium in German bottled and tap water. J. Geochem. Explor. 107, 272–282.

Chabaux, F., Bourdon, B., Riotte, J., 2008. Chapter 3 U-series geochemistry in weathering profiles, river waters and lakes. In: Krishnaswami, S., Cochran, J.K. (Eds.), Radioactivity in the Environment. Elsevier, pp. 49–104.

Cothern, R.C., Lappenbusch, W.L., 1983. Occurrence of uranium in drinking water in the U.S. Health Phys. 45, 89–99.

Cumberland, S.A., Douglas, G., Grice, K., Moreau, J.W., 2016. Uranium mobility in organic matter-rich sediments: a review of geological and geochemical processes. Earth Sci. Rev. 159, 160–185.

Davis, B.A.S., Brewer, S., Stevenson, A.C., Guiot, J., 2003. The temperature of Europe during the Holocene reconstructed from pollen data. Quat. Sci. Rev. 22, 1701–1716.

EDI, 2017. Verordnung des EDI über Trinkwasser sowie Wasser in öffentlich zugänglichen Bädern und Duschanlagen (TBDV). Swiss Federal Department of Home Affairs.

EFSA, 2009. Scientific opinion of the panel on contaminants in the food chain on a request from German federal institute for risk assessment (BfR) on uranium in foodstuff, in particular mineral water. EFSA J. 1018, 1–59.

Eikenberg, J., Beer, H., Jaggi, M., 2014. Determination of ^{210}Pb and ^{226}Ra/^{228}Ra in continental water using HIDEX 300SL LS-spectrometer with TDCR efficiency tracing and optimized alpha/beta-discrimination. Appl. Radiat. Isot. 93, 64–69.

Faure, G., Mensing, T.M., 2005. Isotopes - Principles and Applications. John Wiley & Sons, Hoboken, New Jersey.

Federal Office of Meteorology, Climatology MeteoSwiss, 2019. Monthly and Annual Precipitation Maps. Zürich.

Godoy, J.M., Godoy, M.L., 2006. Natural radioactivity in Brazilian groundwater. J. Environ. Radioact. 85, 71–83.

Gonzalez, Z.I., Krachler, M., Cheburkin, A.K., Shotyk, W., 2006. Saptial distribution of natural enrichements of Arsenic, Selenium and Uranium in a minerotrophic peatland, Gola die Lago, Canton Ticicno, Switzerland. Environ. Sci. Technol. 40, 6568–6574.

Graf, U., Küchler, M., Ecker, K., Feldmeyer-Christe, E., Könitzer, C., Känzig, U., Grosvernier, P., Berchten, F., Lugon, A., David, R., Marti, F., 2007. Zustand und Entwicklung der Moore in der Schweiz - Ergebnisse der Erfolgskontrolle Moorschutz. Bundesamt für Umwelt BAFU Umweltzustand Nr, pp. 1–97.

Horwitz, E.P., Dietz, M.L., Chiarizia, R., Diamond, H., Essling, A.M., Graczyk, D., 1992. Separation and preconcentration of uranium from acidic media by extraction chromatography. Anal. Chim. Acta 266, 25–37.

Ivanovich, M., Harmon, R.S., 1992. Uranium-series Disequilibrium: Applications to Earth, Marine, and Environmental Sciences. Clarendon Press.

Jouvet, G., Seguinot, J., Ivy-Ochs, S., Funk, M., 2017. Modelling the diversion of erratic boulders by the Valais Glacier during the last glacial maximum. J. Glaciol. 63, 487–498.

Keith, L.S., Faroon, O.M., Fowler, B.A., 2015. Uranium, Handbook on the Toxicology of Metals, fourth ed. Academic Press, San Diego, pp. 1307–1345.

Keller, B., 1992. Hydrologie des schweizerischen Molasse-Beckens: aktueller Wissensstand und weiterführende Betrachtungen. Eclogae Geol. Helv. 85, 611–651.

Krachler, M., Shotyk, W., 2004. Natural and anthropogenic enrichments of molybdenum, thorium, and uranium in a complete peat bog profile, Jura Mountains, Switzerland. J. Environ. Monit. 6, 418–426.

Krüger, J.P., Leifeld, J., Glatzel, S., Szidat, S., Alewell, C., 2015. Biogeochemical indicators of peatland degradation – a case study of a temperate bog in northern Germany. Biogeosciences 12, 2861–2871.

L'Annunziata, M.F., 2012. Handbook of Radioactivity Analysis. Academic Press, Amsterdam.

Larock, P., Hyun, J.H., Boutelle, S., Burnett, W.C., Hull, C.D., 1996. Bacterial mobilization of polonium. Geochem. Cosmochim. Acta 60, 4321–4328.

Lee, H.M., Hong, G.H., Baskaran, M., Kim, S.H., Kim, Y.I., 2014. Evaluation of plating conditions for the recovery of ^{210}Po on a Ag planchet. Appl. Radiat. Isot. 90, 170–176.

Li, D., Kaplan, D.I., Chang, H.-S., Seaman, J.C., Jaffé, P.R., Koster van Groos, P., Scheckel, K.G., Segre, C.U., Chen, N., Jiang, D.-T., Newville, M., Lanzirotti, A., 2015. Spectroscopic evidence of uranium immobilization in acidic wetlands by natural organic matter and plant roots. Environ. Sci. Technol. 49, 2823–2832.

Li, D., Seaman, J.C., Chang, H.S., Jaffe, P.R., Koster van Groos, P., Jiang, D.T., Chen, N., Lin, J., Arthur, Z., Pan, Y., Scheckel, K.G., Newville, M., Lanzirotti, A., Kaplan, D.I., 2014. Retention and chemical speciation of uranium in an oxidized wetland sediment from the Savannah River Site. J. Environ. Radioact. 131, 40–46.

Liesch, T., Hinrichsen, S., Goldscheider, N., 2015. Uranium in groundwater - fertilizers versus geogenic sources. Sci. Total Environ. 536, 981–995.

Mason, B.H., Moore, C.B., 1982. Principles of Geochemistry. Wiley, New York.

Matter, A., Homewood, P., Caron, C., Rigassi, D., Stuijvenberg, J.v., Weidmann, M., Winkler, W., 1980. Excursion No. V: Flysch and Molasse of Western and Central Switzerland, Geology of Switzerland - A Guide-Book. Schweizerische Geologische Kommission, Basel, pp. 261–293.

Meija, J., Coplen, T.B., Berglund, M., Brand, W.A., De Bièvre, P., Gröning, M., Holden, N.E., Irrgeher, J., Loss, R.D., Walczyk, T., Prohaska, T., 2016. Isotopic compositions of the elements 2013 (IUPAC technical report). Pure Appl. Chem. 88, 293–306.

Ndiaye, M., Clerc, N., Gorin, G., Girardclos, S., Fiore, J., 2014. Lake neuchâtel (Switzerland) seismic stratigraphic record points to the simultaneous würmian deglaciation of the rhône glacier and Jura ice cap. Quat. Sci. Rev. 85, 1–19.

Osmond, J.K., Cowart, J.B., 1976. The theory and uses of natural uranium isotopic variations in hydrology. Atom. Energy Rev. 14, 621–679.

Osmond, J.K., Cowart, J.B., Ivanovich, M., 1983. Uranium isotopic disequilibrium in ground water as an indicator of anomalies. Int. J. Appl. Radiat. Isot. 34, 283–308.

Pfiffner, O.A., 2014. Geology of the Alps. Wiley.

Ram, R., Vaughan, J., Etschmann, B., Brugger, J., 2019. The aqueous chemistry of polonium (Po) in environmental and anthropogenic processes. J. Hazard Mater. 380, 120725.

Ramseyer, R., 1952. Geologie des Wistenlacherberges (Mont Vully) und der Umgebung von Murten (Kt. Freiburg). Eclogae Geol. Helv. 45 (2).

Reimer, P.J., Bard, E., Bayliss, A., Beck, J.W., Blackwell, P.G., Ramsey, C.B., Buck, C.E., Cheng, H., Edwards, R.L., Friedrich, M., Grootes, P.M., Guilderson, T.P., Haflidason, H., Hajdas, I., Hatté, C., Heaton, T.J., Hoffmann, D.L., Hogg, A.G., Hughen, K.A., Kaiser, K.F., Kromer, B., Manning, S.W., Niu, M., Reimer, R.W., Richards, D.A., Scott, E.M., Southon, J.R., Staff, R.A., Turney, C.S.M., van der Plicht, J., 2013. IntCal13 and Marine13 radiocarbon age calibration curves 0–50,000 Years cal BP. Radiocarbon 55, 1869–1887.

Rybach, L., Bächler, D., Bucher, B., Schwarz, G., 2002. Radiation doses of Swiss population from external sources. J. Environ. Radioact. 62, 277–286.

Rybach, L., Medici, F., Schwarz, G.F., 1997. Construction of radioelement and dose-rate baseline maps by combining ground and airborne radiometric data. In: IAEA TECDOC-980: Uranium Exploration Data and Techniques Applied to the Preparation of Radioelement Maps, pp. 33–45.

Sale, J.W., 1930. Control of mineral waters and their salts under the federal foods and drugs act. Ind. Eng. Chem. 22, 332–335.

Schott, B., Wiegand, J., 2003. Processes of radionuclide enrichment in sediments and ground waters of Mont Vully (Canton Friburg, Switzerland). Eclogae Geol. Helv. 96, 99–107.

Schumann, R.R., Zielinski, R.A., Otton, J.K., Pantea, M.P., Orem, W.H., 2017. Uranium delivery and uptake in a montane wetland, north-central Colorado, USA. Appl. Geochem. 78, 363–379.

Shin, W., Oh, J., Choung, S., Cho, B.-W., Lee, K.-S., Yun, U., Woo, N.-C., Kim, H.K., 2016. Distribution and potential health risk of groundwater uranium in Korea. Chemosphere 163, 108–115.

Sinclair, H.D., Coakley, B.J., Allen, P.A., Watts, A.B., 1991. Simulation of Foreland Basin Stratigraphy using a diffusion model of mountain belt uplift and erosion: an example from the central Alps, Switzerland. Tectonics 10, 599–620.

Stalder, E., Blanc, A., Haldimann, M., Dudler, V., 2012. Occurrence of uranium in Swiss drinking water. Chemosphere 86, 672–679.

Studer, B., 1853. Geologie der Schweiz. Stämpflische Verlagshandlung, Bern.

Swiss Federal Office of Topography, 2019a. Swisstopo Geological Atlas of Switzerland 1. Wabern, pp. 25000.

Swiss Federal Office of Topography, 2019b. Swisstopo Journey through Time Maps. Wabern.

Szidat, S., Salazar, G.A., Vogel, E., Battaglia, M., Wacker, L., Synal, H.A., Türler, A., 2014. ^{14}C analysis and sample preparation at the new bern laboratory for the analysis of radiocarbon with AMS (LARA). Radiocarbon : Int. J. Comput. Intell. Res. 56, 566.

Vesterbacka, P., 2007. Natural radioactivity in drinking water in Finland. Boreal Environ. Res. 12, 11–16.

Wallner, G., Wagner, R., Katzlberger, C., 2008. Natural radionuclides in Austrian mineral water and their sequential measurement by fast methods. J. Environ. Radioact. 99, 1090–1094.

Walsh, M., Wallner, G., Jennings, P., 2014. Radioactivity in drinking water supplies in Western Australia. J. Environ. Radioact. 130, 56–62.

Wang, Y., Bagnoud, A., Suvorova, E., McGivney, E., Chesaux, L., Phrommavanh, V., Descostes, M., Bernier-Latmani, R., 2014. Geochemical control on uranium(IV) mobility in a mining-impacted wetland. Environ. Sci. Technol. 48, 10062–10070.

Werthmüller, S., Surbeck, H., Ryser, R., 2015. Airborne Exploration of Anomalous High Uranium Contents in Water and Soil in the Region of the “Lyssbach” – Canton of Bern. Swiss Geoscience Meeting, Basel.

WHO, 2011. Guidelines for Drinking-Water Quality.

Wu, Y., Wang, Y., Xie, X., 2014. Occurrence, behavior and distribution of high levels of uranium in shallow groundwater at Datong basin, northern China. Sci. Total Environ. 472, 809–817.